



Experimental Study on Mechanical Properties of Sandstone Under Sinusoidal Dynamic Load

Boxue Fu · Dongming Zhang · Chen Ye

Received: 27 July 2021 / Accepted: 24 November 2021 / Published online: 28 January 2022
© The Author(s), under exclusive licence to Springer Nature Switzerland AG 2021

Abstract To investigate the dynamic characteristics of rock, uniaxial sinusoidal stress cyclic loading was applied to a cylindrical sandstone and unloading tests were carried out under different cyclic amplitude, cyclic frequency, and cyclic mean value using a dynamic loading test device, which has been independently developed by Chongqing University. The mechanical properties of sandstone were quantitatively analyzed by considering the elastic modulus and Poisson's ratio. From the viewpoint of energy, the stress–strain diagram of a single cyclic load was divided into different zones, the energy dissipation rate of a complete cycle was defined, and the energy conversion of rock during cyclic loading and unloading was investigated. The following conclusions were drawn. First, the elastic modulus increases with the cyclic amplitude, cyclic mean value, and cyclic frequency of the cyclic loading. This indicates that ultra-high loading and excessively fast frequency cyclic loading will cause the compaction of fine cracks, which leads to the deformation capacity of the

rock being significantly diminished. Secondly, under cyclic loading, there is a cut-off point for the cyclic amplitude, cyclic frequency, and cyclic mean value, which results in the obvious fluctuation of Poisson's ratio. This point can be considered as the critical point of rock instability. Finally, in the case of different cyclic amplitude, cyclic frequency, and cyclic mean value, the total work of loading changes only slightly with the number of cycles, and the energy dissipation rate is positively correlated with the cyclic amplitude, cyclic mean value, and cyclic frequency.

Keywords Cyclic load · Sinusoidal stress · Dynamic mechanical parameters · Energy characteristics

1 Introduction

In practical rock engineering applications, the rock mass mostly bears periodic loading. Relevant examples include the rock mass involved in the excavation of the slope of a dam pier, the excavation and support of an underground cavern, geological tectonic movement, and the foundation of a powerhouse with large power equipment. Therefore, it is necessary to investigate the mechanical properties of rock in the process of cyclic loading and unloading so as to ensure stable operation over a long period of time for projects such as those mentioned above.

B. Fu · D. Zhang (✉) · C. Ye
School of Resources and Safety Engineering, Chongqing University, Chongqing 400044, China

B. Fu · D. Zhang · C. Ye
State Key Laboratory of Coal Mine Disaster Dynamics and Control, Chongqing University, Chongqing 400044, China

To this end, extensive research has been conducted in recent years. Li et al. (2019a, b) conducted two sets of circulating load tests and clarified the deformation characteristics of rock under circulating loading, the elastic modulus of the fissure rock body, and the development law of residual strain. Liu et al. (2018) systematically investigated the fatigue mechanical properties of the artificial-joint rock model under different circulation conditions indoors, and described the influence of three circulation load parameters on the fatigue deformation characteristics, fatigue energy, and damage development. Rashid et al. (2019) investigated the effects of circulating load on the fatigue life, deformation characteristics, and damage mechanism of two different rocks with microstructure through uniaxial monotonic and cyclic compression tests. Li et al. (2019a, b) proposed a constitutive model to predict the shear behavior of rock joints under cyclic loading. Based on the results obtained by a dynamic triaxial test at the frequency of 1.0 Hz, Liu and Liu (2017) analyzed the stress amplitude of artificial-joint rocks with different joint inclination angles and their mechanical behavior under different enclosures. Lin et al. (2020) investigated the mechanical properties of a bifurcated-joint rock body under uniaxial loading using the discrete element method. Meng et al. (2016) investigated the effects of different joint parameters on the strength and fracture behavior of a double-circle-joint rock body. They investigated thirty sandstone specimens circulated around the order axis at six different loading velocities to characterize the energy storage, evolution, and dissipation during the compression uninstillation process, and analyzed the stress–strain relationship and acoustic emission characteristics of the deformation fracture of rock samples. Moreover, they confirmed the densities and velocities of energy storage, and the elastic and dissipative energies at different load velocities, and proposed effective methods for solving the equivalent energy plane. Li et al. (2020) investigated the anisotropic fatigue behavior of shale and performed uniaxial fatigue tests at different circulating stress limits and loading frequencies using seven different stratified shale tests. They analyzed the fatigue fracture mechanism, stress strain behavior, number of cycles, irreversible strain, and anisotropic characteristics of the energy development of each hysteresis loop. Through a series of laboratory tests, Liu and He (2012) investigated the

effect of scale pressure on the mechanical properties of sandstone under cycling loading and the development of fatigue damage. Peng et al. (2019) conducted a conventional 3-axis compression test, a 3-axis circulation loading test with a lower stress limit, and a 3-axis circulation loading test with a lower constant stress limit, and then investigated the impact on the lower limit of the circulation stress in the characteristics and rules of sandstone deformation. Shen et al. (2020) tested sandstone samples with different stress paths under circulating loading and uninstillation, and analyzed the changes in the mechanical properties and acoustic radiation signals of the sample during cyclic loading and uninstillation. Based on experimental data, Wang et al. (2020) proposed a damage development model describing the two-step fatigue accumulation characteristics. Their work shed more light on the fatigue damage mechanism of rocks under multi-stage fatigue loading. Through the test results and analysis of the circulating load phenomenon, Zheng et al. (2020) found that the frequency significantly affects the power characteristics of the nodal body. Liu et al. (2012) investigated the effect of frequency on the circulating loading power characteristics of sandstone samples under ambient pressure through a series of laboratory tests. The results obtained by the cyclic loading test reveal that the frequency greatly influences the dynamic deformation, dynamic rigidity, and fracture mode under the same ambient pressure. Lin et al. (2020) conducted a series of uniaxial compression tests on non-permanent joint rock bodies with bi-circular holes. The tests revealed that the presence of non-permanent joints significantly affects the strength characteristics of the test piece. Cao et al. (2020) performed a uniaxial compression test on a cubic rock prototype containing non-persistent joints (in-plane) and further investigated the joint inclination angle θ and the durability N 's effect on the mechanical and fracture properties of rocks. Lin et al. (2020) conducted fatigue damage tests on Huangyan samples and found that, as the number of cycles increased, Young's modulus gradually stabilized but the delineation rate decreased non-linearly. Jafari et al. (2004) introduced the mechanical properties of artificial rock joints in circular shearing action. Yan et al. (2020) used a Hopkinson squeezer to perform a dynamic compression test on a rock test piece with multiple parallel cracks. The final fracture mode for all samples was the X-shaped shear fracture mode, regardless of the crack

strength. Zhao et al. (2017) performed triaxial creep tests on full and crack test pieces in a multi-level loading and unloading cycle. The results reveal that the viscoelastic strain tended to become constant with time. However, the viscoelastic strain increased with time and tended to increase with the bias voltage. Ghamgosar et al. (2017) investigated different FPZ modes at different circulating loads and quantitatively defined the damage and fracture patterns by the particle or rock matrix.

By considering the Hopkinson and exfoliation phenomenon, Cho et al. (2003) conducted dynamic tensile tests on granite and tuff, and investigated the strain rate dependence of the dynamic tensile strength of rock. Asprone et al. (2008) investigated the influence of highly dynamic loading conditions on a typical porous natural rock in the Naples area, in Italy. The dynamic growth factor (DIFS) and strain rate curve of the tensile failure stress were evaluated and discussed. Bagde and Petroš (2008) introduced the fatigue behavior of the explosive sandstone samples of mining rocks under dynamic uniaxial cycling loading. They tested dry saturated samples at 0.1 Hz, 1 Hz, and 10 Hz with the amplitude of 0.05 mm, 0.1 mm, and 0.15 mm. Through laboratory experiments, they found that the load frequency and amplitude have important implications for rock behavior under dynamic circulating load conditions. Tutuncu et al. (2012) conducted uniaxial stress cycling experiments on dry, brine-saturated, and cetane-saturated belia sandstone samples, observed the hysteresis phenomenon in the stress–strain diagram in detail, and elucidated the influence of different fluids on the elastic modulus and attenuation of strain amplitude dependence.

In summary, domestic and overseas research on dynamic loading has mainly focused on triangular waves or square waves, and research on the mechanical properties of rock under sinusoidal stress is insufficient. This study carried out uniaxial cyclic loading and unloading experiments on sandstone obtained from Chongqing Metro Line 9 under sine wave loading with different stress cyclic amplitude, cyclic frequency, and cyclic mean value, and obtained the stress–strain curve and local strain under uniaxial sinusoidal stress.

2 Testing Scheme and Equipment

2.1 Sample Preparation

All experimental rock samples were obtained from Chongqing Metro Line 9 and processed into cylindrical standard parts (100 × 50 mm) in the laboratory according to the experimental research protocol. Finally, the end face of the specimen was polished to become smooth, and the length was controlled at 100 ± 1 mm. To measure the local strain of the sample during the test, a strain gauge with orthogonal configuration was installed at the center of the sample. The experimental process is shown in Fig. 1.

To ensure the accuracy of the test results and reduce random error, the rock samples were observed with naked eyes to check whether the rock samples are universal. Then, CT scanning was used to observe whether obvious cracks existed inside the samples. Owing the homogeneity of sandstone, most sandstones satisfied the test standards. The CT scanning results are presented in Fig. 2. The average length, diameter, density, uniaxial compressive strength, elastic modulus, and Poisson's modulus of the test sandstone specimens are listed in Table 1. The data were acquired from the average test results obtained for six specimens selected in advance.

2.2 Testing Scheme

As shown in Fig. 3, a servo-controlled testing machine, which has been independently developed by Chongqing University (Patent No. ZL201910282368.4), was used to carry out uniaxial compression tests in displacement-controlled deformation mode. During the entire deformation process, the axial displacement and stress were recorded by a central computer at the same sampling frequency. Additionally, the Sigmar ASMD3-16 strain gauge was used to measure the strain gauge data.

The technical parameters of the equipment are as follows:

- (1) Vertical load (static): 1500 KN.
- (2) Maximum stroke of oil cylinder piston: 150 mm.
- (3) Frequency of dynamic actuator: 0.01–10 Hz.
- (4) Dynamic actuator amplitude: ± 5 mm at 2 Hz.
- (5) Testing method: closed loop control of load and displacement.

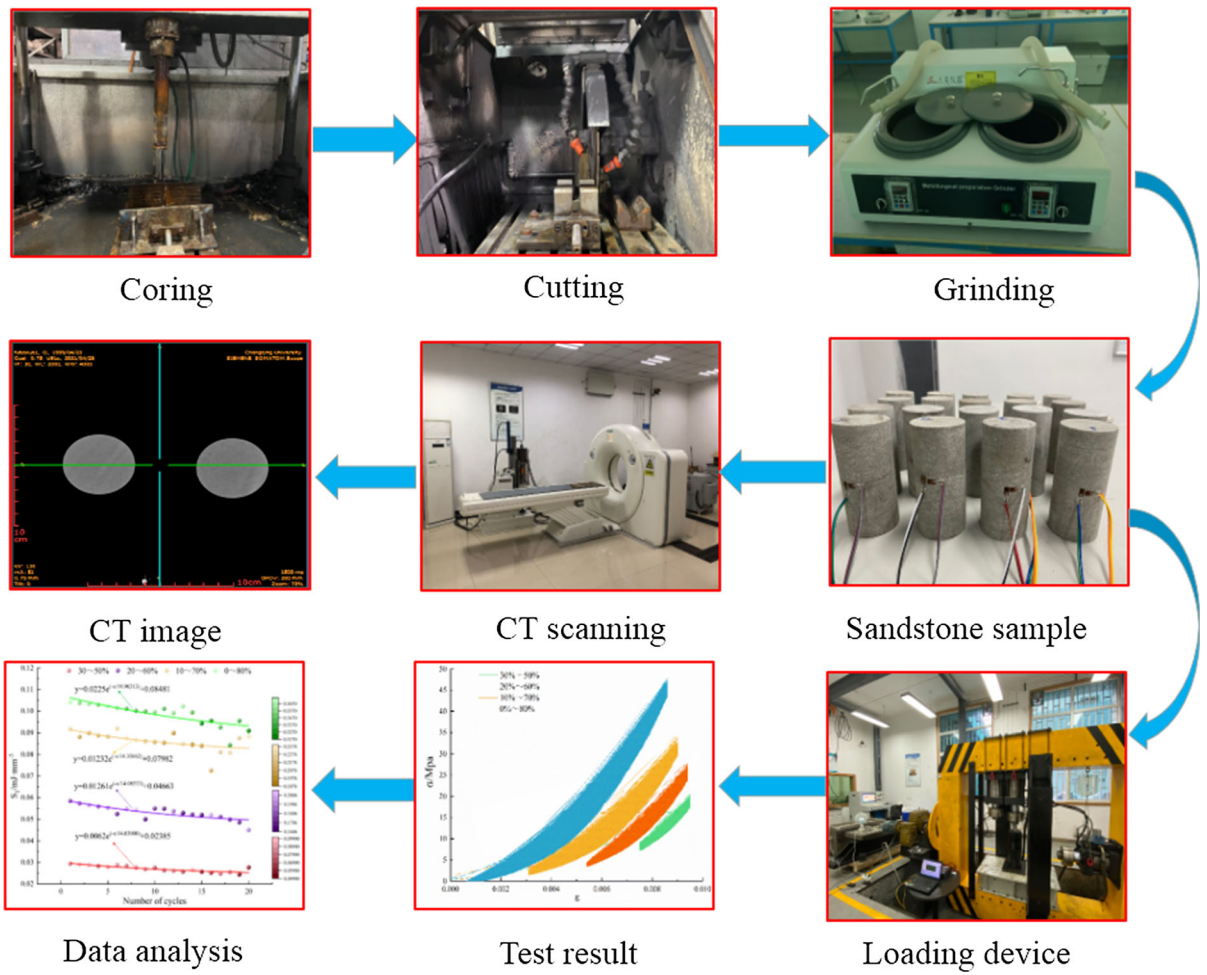


Fig. 1 Experimental process

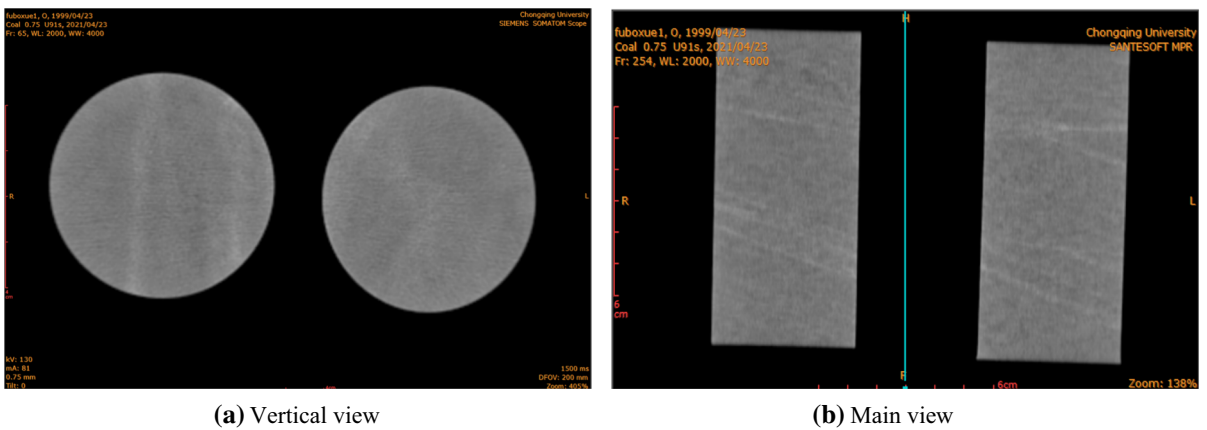


Fig. 2 CT image **a** Vertical view **b** Main view

Table 1 Average value of basic parameters

Name / Unit	L/mm	d/mm	$\rho/\text{kg}\cdot\text{m}^{-3}$	σ_c/MPa	E/GPa	ν
Average value of basic parameters	101.2	49.55	2499.54	43.97	2.56	0.25

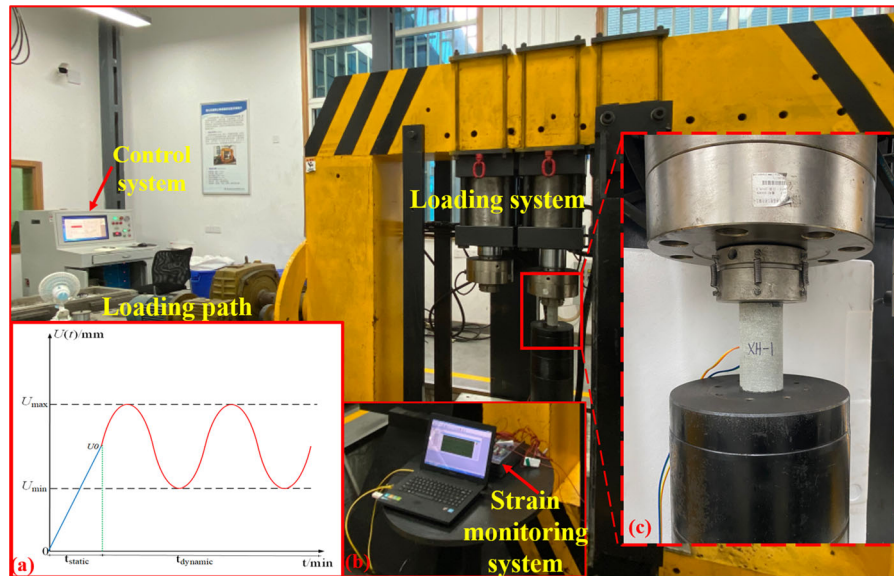


Fig. 3 Test apparatus: **a** Loading path **b** Strain monitoring **c** Sandstone sample

(6) Test waveform: sine wave, square wave, triangular wave, and static step loading.

The specific testing scheme is as follows:

Scheme 1: Investigate the influence of cyclic loading and unloading with different load amplitudes on the rock damage and deformation. The vertical dynamic loading frequency is 0.5 Hz, the mean stress cyclic value is 40% of the uniaxial compressive strength, the cyclic amplitudes are 10%, 20%, and 30% of the uniaxial compressive strength, respectively, and the loading duration is maintained for 30 min

Scheme 2: Investigate the influence of the cyclic loading and unloading frequency on the rock damage and deformation. The cyclic mean value is 40% of the uniaxial compressive strength, the load amplitude is 20% of the uniaxial compressive strength, the load frequency changes to 0.2 Hz, 0.4 Hz, 0.6 Hz, and 0.8 Hz, respectively, and the loading duration is maintained for 30 min

Scheme 3: Investigate the influence of cyclic loading and unloading with different mean cyclic stress on the rock damage and deformation. The cyclic stress amplitude is 40% of the uniaxial compressive strength, the cyclic frequency is 0.5 Hz, the mean cyclic stress is 20%, 40%, 60%, and 80% of the uniaxial compressive strength, and the loading time is 30 min

3 Analysis of Test Results

To analyze the mechanical properties of sandstone specimens under dynamic loading, the elastic modulus, Poisson’s ratio and dissipated energy were selected for analysis.

3.1 Analysis of Elastic Modulus

Figure 4 shows the stress–strain curves obtained for the sandstone samples under different cyclic amplitude, frequency, and mean value.

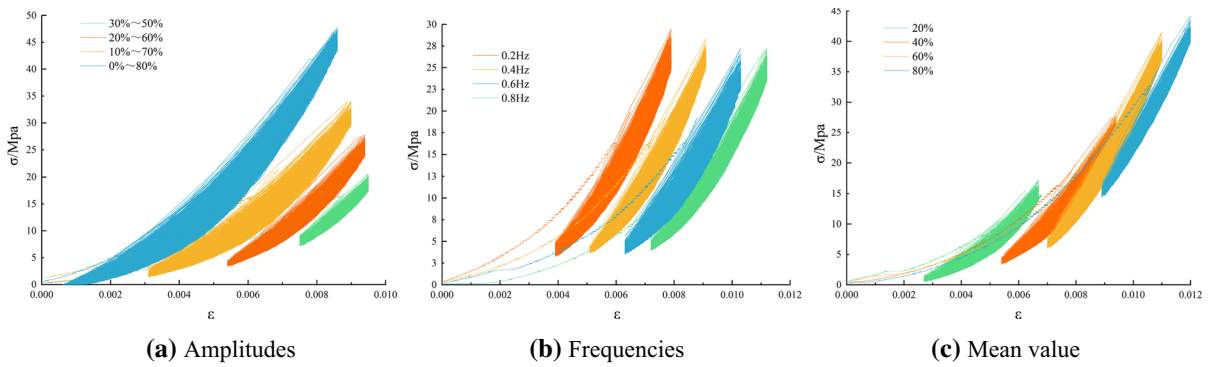


Fig. 4 Stress strain diagram under different conditions **a** Amplitudes **b** Frequencies **c** Mean value

As shown in Fig. 4a, when the other test conditions are the same, the cyclic level of 0%–80% is on the leftmost side, while that of 30%–50% is on the rightmost side. As the cyclic amplitude decreases, the stress–strain curves are arranged from left to right. As shown in Fig. 4b, as the frequency increases, the stress–strain curves are arranged from left to right. In Fig. 4c, as the cyclic mean value increases, the stress–strain curves are arranged from left to right.

From the 0%–80% curve in Fig. 4a, it can be seen that the maximum stress is greater than 45 MPa, which exceeds the average uniaxial compressive strength. There are two reasons for this. First, the heterogeneity of the rock results in different maximum compressive strength for each rock sample. Second, the displacement-controlled loading mode adopted in this test cannot perfectly control the peak amplitude to 80% of the uniaxial compressive strength.

The slope of the elastic deformation stage of each loading cycle was selected as the dynamic elastic modulus of this cycle to obtain the change rule of the dynamic elastic modulus with the number of cycles under different loading conditions, as shown in Fig. 5.

From Fig. 5, the following observations can be made:

(1) Single factor analysis reveals that the dynamic elastic modulus is positively correlated with the cyclic amplitude, frequency, and mean value. This is mainly because, within the bearing range of rock, the increasing cyclic amplitude, cyclic mean value, and cyclic loading frequency lead to the compaction of fine cracks, and the deformation capacity of rock significantly diminishes.

(2) By comparing the three influencing factors, namely, the cyclic amplitude, cyclic frequency, and cycle mean, it can be seen that the dynamic elastic modulus of each cycle is different but always fluctuates around the mean value.

(3) It can be found that the mean value of the dynamic elastic modulus has a linear relationship with the number of cycles. The fitting relationship between the mean value of the dynamic elastic modulus and the cyclic amplitude, cyclic frequency, and cyclic mean is expressed as follows:

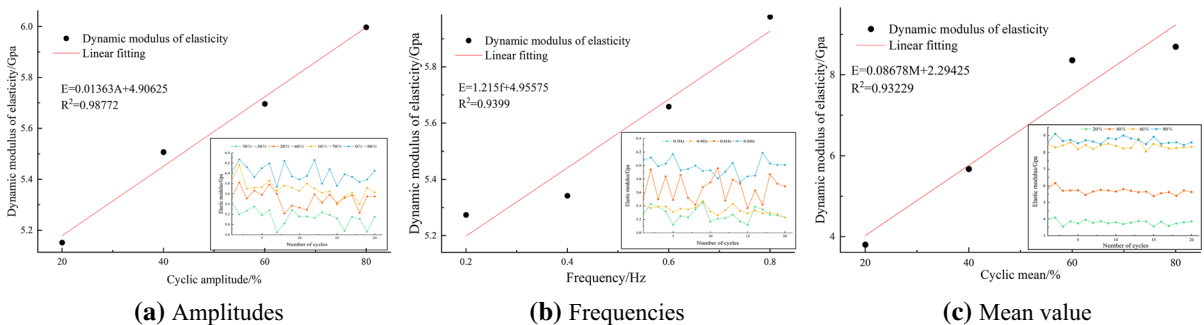


Fig. 5 Dynamic elastic modulus change and linear fitting **a** Amplitudes **b** Frequencies **c** Mean value

$$\begin{cases} E = 0.01363A + 4.90625, R^2 = 0.98772 \\ E = 1.215f + 4.95575, R^2 = 0.9399 \\ E = 0.08678M + 2.29425, R^2 = 0.93229 \end{cases} \quad (1)$$

where A represents cyclic amplitude, f represents cyclic frequency, and M represents cyclic mean.

3.2 Poisson’s Ratio

The local strain of each rock sample in the process of cyclic loading and unloading was measured from the strain gauge data, and the ratio of the transverse strain to the axial strain is Poisson’s ratio. The calculation data are presented in Fig. 6.

From Fig. 6, the following observations can be made:

(1) Under different stress cyclic amplitudes, the amplitude variance from small to large is 3.828×10^{-6} , 6.54×10^{-6} , 6.16×10^{-6} , and 1.092×10^{-5} . As can be seen, Poisson’s ratio greatly fluctuates when the amplitude is 40%. As the cyclic amplitude increases, Poisson’s ratio becomes smaller.

(2) Under different loading frequencies, the frequency variance from high to low is 2.174×10^{-5} , 1.07×10^{-5} , 4.64×10^{-4} , and 2.01×10^{-3} . This indicates that the influence of high-frequency cyclic loading and unloading on Poisson’s ratio is obvious. Additionally, when the other conditions are consistent, the frequency is lower and the Poisson’s ratio is smaller.

(3) When the other loading environments are consistent, the variance of the mean value, from large to small, is 1.07×10^{-4} , 6.54×10^{-6} , 4.49×10^{-5} , and 6.18×10^{-5} . As can be seen, a low cyclic mean value greatly influences Poisson’s ratio, and as the

cyclic mean value decreases, Poisson’s ratio becomes smaller.

4 Research on Energy Dissipation

Energy loss is an important rock attribute in the process of deformation and failure, and reflects the continuous closure process of micro defects in rock, and the development and evolution of new fractures. The strength of the material continuously decreases and finally loses its strength. Therefore, the mechanical response characteristics of rock can be better explained from the viewpoint of energy. Figure 7 shows the schematic diagram of the energy within a single cycle.

The energy in a cycle is determined by the following relationship:

$$S_1 = S_2 + S_3, \quad (2)$$

where S_1 represents the total absorbed energy (mJ/mm^3), S_2 represents the elastic potential energy released in the unloading process of the rock (mJ/mm^3), and S_3 represents the energy consumed in one cycle (mJ/mm^3).

Notably, S_3 is used for the friction sound and heat of the particles in the rock, the increase of the rock’s own micro cracks, and the generation of new cracks.

$$S_1 = \int_{\epsilon'_t}^{\epsilon''_t} \sigma_1 d\epsilon, \quad (3)$$

$$S_2 = \int_{\epsilon'_t}^{\epsilon''_t} \sigma_2 d\epsilon, \quad (4)$$

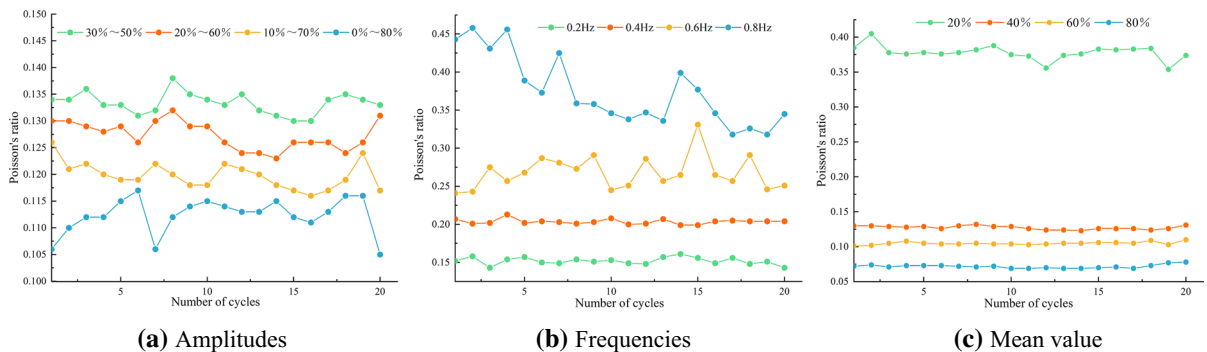


Fig. 6 Curves of Poisson’s ratio under different conditions **a** Amplitudes **b** Frequencies **c** Mean value

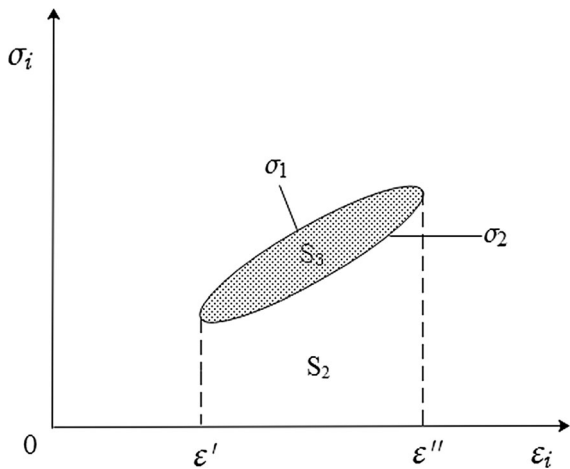


Fig. 7 Energy analysis diagram under single-cycle loading and unloading

The energy dissipation rate S_3/S_1 is defined as the ratio of the consumed energy S_3 to the total S_1 of the upper external force. The energy parameters (S_1 , S_3/S_1) under different conditions are shown in Figs. 8, 9, and 10.

As shown in Fig. 8, under different cyclic loading and unloading amplitudes, the work done by each

cycle on the rock (S_1) fluctuates upward and downward, but generally decreases. It can be found that the total work under each condition has a linear relationship with the number of cycles. The fitting curves are as follows:

$$\begin{cases} y = 0.0225e^{(-x/19.96313)} + 0.08481 \\ y = 0.01232e^{(-x/14.35662)} + 0.08481 \\ y = 0.01261e^{(-x/14.08533)} + 0.04663 \\ y = 0.0062e^{(-x/14.03008)} + 0.02385 \end{cases} \quad (5)$$

In the figure, the energy dissipation rate is represented by the color of the ball. As the color becomes deeper, the energy dissipation rate becomes lower. According to the color of the ball, it can be seen that the dissipation rate exhibits a decreasing trend under the same conditions. Moreover, it can be seen that, as the amplitude of the cycle increases, the energy dissipation rate becomes greater provided that the other cyclic loading and unloading test conditions are unchanged.

As shown in Fig. 9, the total work done on the rock varies with the number of cycles. Under different amplitude conditions, both energy parameters fluctuate but eventually exhibit a downward trend. The

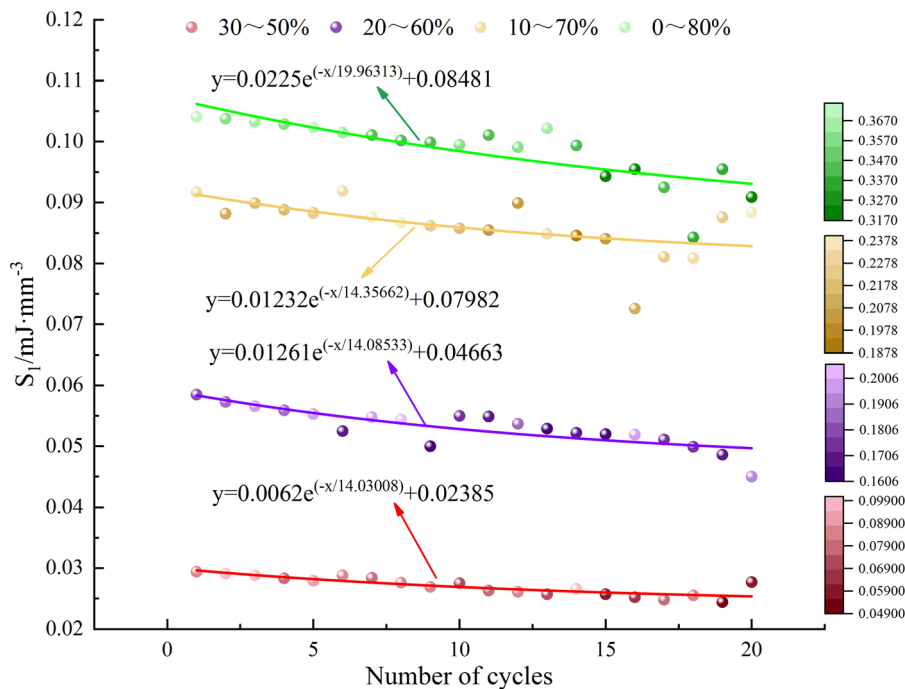


Fig. 8 Curves of energy parameters under different cyclic amplitude

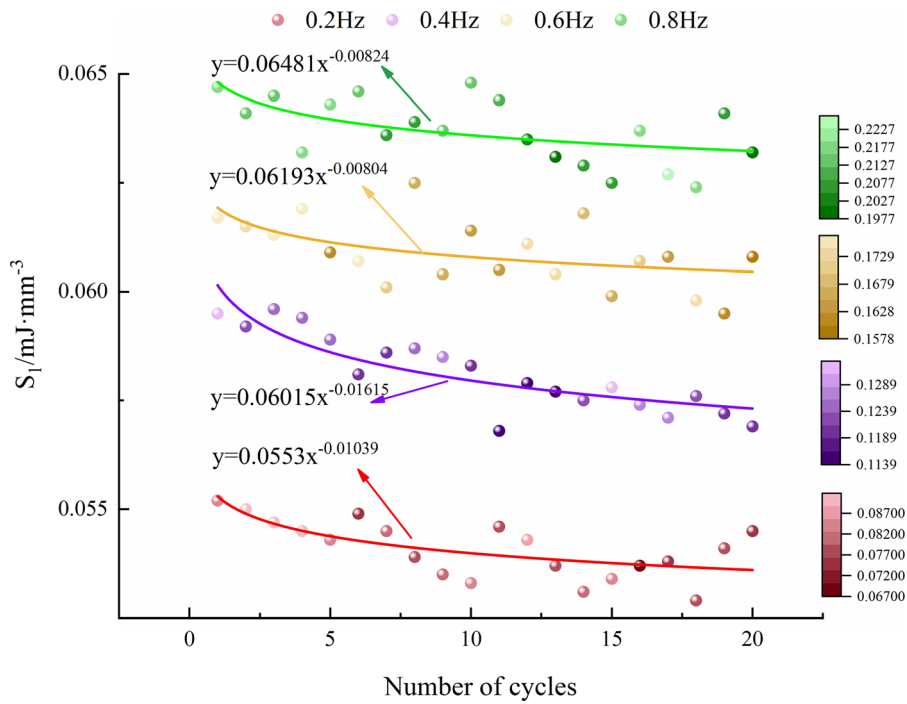


Fig. 9 Curves of energy parameters under different loading frequencies

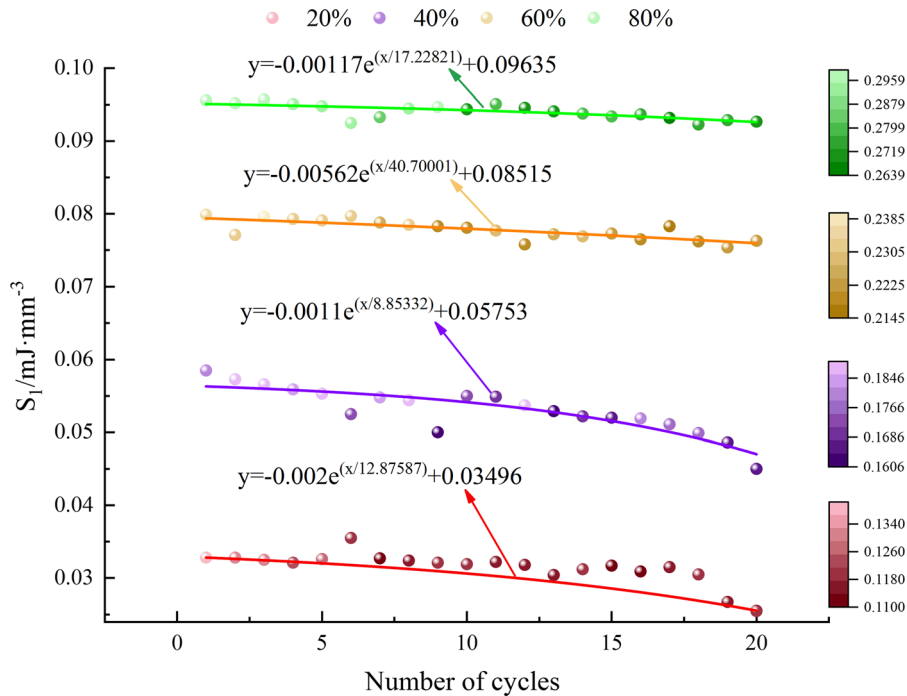


Fig. 10 Curves of energy parameters under different mean cyclic loading values

fitting curves of the total work and cycle times under different conditions are as follows:

$$\begin{cases} y = 0.06481x^{-0.00824} \\ y = 0.06193x^{-0.00804} \\ y = 0.06015x^{-0.01615} \\ y = 0.0553x^{-0.01039} \end{cases} \quad (6)$$

As can be seen, the energy dissipation rate exhibits a downward trend and obviously changes with the frequency. Moreover, the energy dissipation rate becomes higher as the frequency increases.

As shown in Fig. 10, under the average value of different cyclic loads, the work done by each cycle to the rock (S_1) varies with the number of cycles, and its change is very small but still exhibits a downward trend. The fitting curves of the total work and cycle times under different conditions are as follows:

$$\begin{cases} y = -0.00117e^{(x/17.22821)} + 0.09635 \\ y = -0.00562e^{(x/40.70001)} + 0.08515 \\ y = -0.0011e^{(x/8.85332)} + 0.05753 \\ y = -0.002e^{(x/12.87587)} + 0.03496 \end{cases} \quad (7)$$

The results are consistent with the two above-mentioned conditions, and the energy dissipation rate exhibits a downward trend. In terms of the energy dissipation rate, as the cyclic mean value increases, the energy dissipation rate becomes greater.

An overall analysis of the three figures shows that, under the condition of uniaxial cyclic loading and unloading, the work done by each cycle to rock tends to decline, which means that the rock tends to be dense under each loading. In this test, displacement-controlled cyclic loading and unloading was adopted; therefore, less work is done to the rock by each cycle.

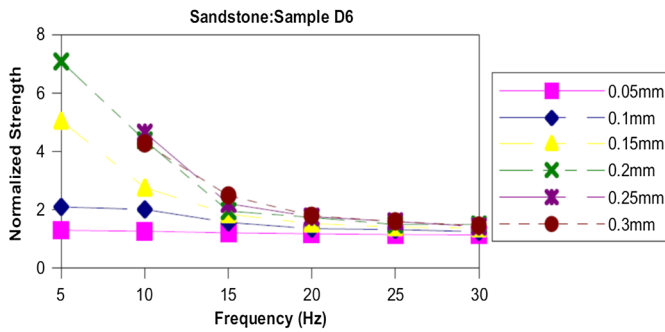
5 Discussion

In this study, the sinusoidal curve was used as the loading mode for fine sandstone. The evolution law of the hysteretic curve of the fine sandstone samples under periodic loading was obtained under four loading amplitudes, loading frequencies, and mean loading values. Then, the dynamic elastic modulus, Poisson's ratio, and the energy characteristics of the fine sandstone samples under periodic loading were analyzed. The test results have certain significance in terms of revealing the mechanical properties and damage mechanism of fine sandstone under dynamic

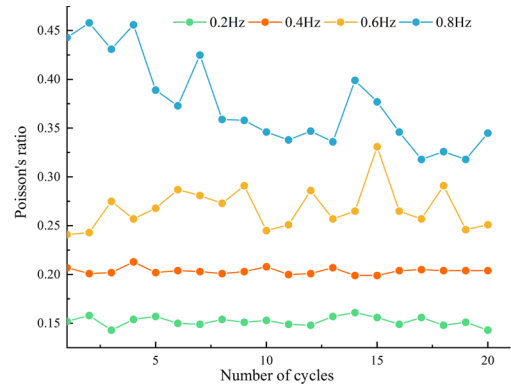
loading. However, the research object of this study is limited to fine sandstone with good homogeneity. Hence, it is necessary to investigate whether other rock types with severe internal initial damage are generally applicable, and their role in geotechnical engineering should also be assessed. For a long time, the rock strength and failure criterion based on classical elastic–plastic theory have been the basis for assessing engineering damage or failure. However, as a description of a specific mechanical state, the stress–strain is only one aspect of the thermodynamic state of rock. The stress–strain curve and rock strength obtained by laboratory testing have great discreteness, and even similar samples obtained from the same rock will be different. Additionally, engineering calculation can introduce errors caused by inaccurate parameter selection. This imposes various restrictions to the engineering design and accurate evaluation of safety.

Bagde and Petroš (2009) introduced the fatigue behavior of sandstone under dynamic uniaxial cyclic loading. As shown in Fig. 11a, they used normalized strength to indicate whether the rock is unstable under different loading frequencies. Instead, this study used the amplitude of the fluctuation of Poisson's ratio, as shown in Fig. 11b. Although expressed in different ways, the obtained laws are similar. Under high-frequency vibration, it can be found that the rock will have lower strength and lose stability. It can also be found that, under three different cyclic conditions, there are critical conditions resulting in the obvious fluctuation of the Poisson's ratio curve. Therefore, in this study, the cyclic amplitude, frequency, and mean value under these conditions were considered as the critical point of rock instability.

In this study, the test was controlled using the displacement loading mode, while the load control mode was not used. The reason for this is that, when the rock reaches the ultimate strength and fails entirely, the actuator will follow the deformation of the specimen to produce a large displacement and maintain the set load level. In other words, a large amount of energy is input within a short time, which intensifies the damage to the sample. In this study, displacement control could avoid the stress release caused by sudden rock failure and facilitate the better investigation of the sample's damage process under dynamic loading. The disadvantage of this approach is that the stress state at the upper and lower peak during the cycle cannot be kept constant.



(a) Normalized strength with frequency (Bagde and Petroš (2009))



(b) Poisson's ratio with frequency

Fig. 11 Different methods for analyzing rock instability **a** Normalized strength with frequency((Bagde and Petroš, 2004)) **b** Poisson's ratio with frequency

6 Conclusion

In this paper, according to the change of the physical parameters of rock under cyclic loading, uniaxial sinusoidal stress cyclic loading and unloading tests were carried out under different cyclic amplitude, cyclic frequency, and cyclic mean value. The results are as follows:

- (1) When the stress does not reach the maximum compressive strength and the other loading conditions are the same, the elastic modulus increases with the amplitude, mean value, and frequency of cyclic loading. This indicates that a larger amplitude, mean value, and frequency of cyclic loading will result in the compaction of micro cracks and the diminishing of the rock's deformation capacity.
- (2) In the three considered testing schemes, when the cyclic amplitude is 40%, Poisson's ratio greatly fluctuates compared with the other amplitude conditions. When the frequency is greater than or equal to 0.6 Hz, Poisson's ratio obviously fluctuates. When the cyclic mean value is 20%, the fluctuation is relatively obvious. The cyclic amplitude, cyclic frequency, and cyclic mean can be considered as the boundary point of rock instability.
- (3) The work done by each cycle to rock, the elastic potential energy released by the rock, and the consumed energy can be determined by decomposing the stress–strain diagram of cyclic loading and unloading, and the energy dissipation

rate of a cycle can be defined. Under the condition of different cyclic amplitude, frequency, and mean value, the work done by loading causes little change to the number of cycles. Additionally, it was found that the energy dissipation rate is positively correlated with the amplitude, mean value, and frequency of cyclic loading.

Acknowledgements This study was supported by Scientific Research Foundation of State Key Laboratory of Coal Mine Disaster Dynamics and Control (Grant No. 2011DA105287-zd201804), this study was financially supported by the National Natural Science Foundation of China (51874053).The authors declare that they have no known competing financial interests or personal relationships that could have appeared to influence the work reported in this paper.

References

Asprone D, Cadoni E, Prota A, Manfredi G (2008) Dynamic behavior of a Mediterranean natural stone under tensile loading. *Int J Rock Mech Min* 46:514–520

Bagde MN, Petroš V (2004) Fatigue properties of intact sandstone samples subjected to dynamic uniaxial cyclical loading. *Int J Rock Mech Min* 42:237–250

Bagde MN, Petroš V (2008) Fatigue and dynamic energy behaviour of rock subjected to cyclical loading. *Int J Rock Mech Min* 46:200–209

Cho SH, Ogata Y, Kaneko K (2003) Strain-rate dependency of the dynamic tensile strength of rock. *Int J Rock Mech Min* 40:763–777

Cao R, Yao R, Meng J, Lin Q, Lin H, Li S (2020) Failure mechanism of non-persistent jointed rock-like specimens under uniaxial loading: Laboratory testing. *Int J Rock Mech Min* 132:104341

- Ghamgosar M, Erarslan N, Williams DJ (2017) Experimental investigation of fracture process zone in rocks damaged under cyclic loadings. *Exp Mech* 57:97–113
- Jafari MK, Pellet F, Boulon M, Hosseini KA (2004) Experimental study of mechanical behaviour of rock joints under cyclic loading. *Rock Mech Rock Eng* 37:3–23
- Liu E, Huang R, He S (2012) Effects of frequency on the dynamic properties of intact rock samples subjected to cyclic loading under confining pressure conditions. *Rock Mech Rock Eng* 45:89–102
- Liu E, He S (2012) Effects of cyclic dynamic loading on the mechanical properties of intact rock samples under confining pressure conditions. *Eng Geol* 125:81–91
- Liu M, Liu E (2017) Dynamic mechanical properties of artificial jointed rock samples subjected to cyclic triaxial loading. *Int J Rock Mech Min* 98:54–66
- Liu Y, Dai F, Dong L, Xu N, Feng P (2018) Experimental investigation on the fatigue mechanical properties of intermittently jointed rock models under cyclic uniaxial compression with different loading parameters. *Rock Mech Rock Eng* 51:47–68
- Li T, Pei X, Wang D, Huang R, Tang H (2019a) Nonlinear behavior and damage model for fractured rock under cyclic loading based on energy dissipation principle. *Eng Fract Mech* 206:330–341
- Li Y, Wu W, Tang C, Liu B (2019b) Predicting the shear characteristics of rock joints with asperity degradation and debris backfilling under cyclic loading conditions. *Int J Rock Mech Min* 120:108–118
- Lin Q, Cao P, Cao R, Lin H, Meng J (2020) Mechanical behavior around double circular openings in a jointed rock mass under uniaxial compression. *Arch Civ Mech Eng* 109:102692
- Li C, Gao C, Xie H, Li N (2020) Experimental investigation of anisotropic fatigue characteristics of shale under uniaxial cyclic loading. *Int J Rock Mech Min* 130:104314
- Lin Q, Ping C, Jingjing M, Rihong C, Zhiye Z (2020) Strength and failure characteristics of jointed rock mass with double circular holes under uniaxial compression: insights from discrete element method modelling. *Theor Appl Fract Mec* 109:1–18
- Lin Q, Cao P, Mao S, Ou C, Cao R (2020) Fatigue behaviour and constitutive model of yellow sandstone containing pre-existing surface crack under uniaxial cyclic loading. *Theor Appl Fract Mec* 109:102776
- Meng Q, Zhang M, Han L, Pu H, Nie T (2016) Effects of acoustic emission and energy evolution of rock specimens under the uniaxial cyclic loading and unloading compression. *Rock Mech Rock Eng* 49:81–91
- Peng K, Zhou J, Zou Q, Zhang J, Wu F (2019) Effects of stress lower limit during cyclic loading and unloading on deformation characteristics of sandstones. *Constr Build Mater* 217:202–215
- Vaneghi RG, Thoeni K, Dyskin AV, Sharifzadeh M, Sarmadivaleh M (2020) Fatigue damage response of typical crystalline and granular rocks to uniaxial cyclic compression. *Int J Fatigue* 138:105667
- Shen R, Chen T, Li T, Li H, Fan W, Hou Z, Zhang X (2020) Study on the effect of the lower limit of cyclic stress on the mechanical properties and acoustic emission of sandstone under cyclic loading and unloading. *Theor Appl Fract Mec* 108:102661
- Tutuncu AN, Podio AL, Gregory AR, Sharma MM (2012) Nonlinear viscoelastic behavior of sedimentary rocks, Part I: effect of frequency and strain amplitude. *Geophysics* 63:195–203
- Wang Y, Gao SH, Li CH, Han JQ (2020) Investigation on fracture behaviors and damage evolution modeling of freeze-thawed marble subjected to increasing-amplitude cyclic loads. *Theor Appl Fract Mec* 109:102679
- Yan Z, Dai F, Liu Y, Du H (2020) Experimental investigations of the dynamic mechanical properties and fracturing behavior of cracked rocks under dynamic loading. *B Eng Geol Environ* 79:1–18
- Zhao Y, Zhang L, Wang W, Wan W, Li S, Ma W, Wang Y (2017) Creep behavior of intact and cracked limestone under multi-level loading and unloading cycles. *Rock Mech Rock Eng* 50:1–18
- Zheng Q, Liu E, Sun P, Liu M, Di Yu (2020) Dynamic and damage properties of artificial jointed rock samples subjected to cyclic triaxial loading at various frequencies. *Int J Rock Mech Min* 128:104243

Publisher's Note Springer Nature remains neutral with regard to jurisdictional claims in published maps and institutional affiliations.